Article ID: 1003－6326(2003)02－0431－07

Coupled computation method of physics fields in aluminum reduction cells①

ZHOU Nai-jun(周乃君), MEI Chi(梅 炽), JIANG Chang-wei(姜昌伟),
ZHOU Ping(周 萍), LI Jie(李 [illegible])
(Institute of Simulation and Optimization on Pyro-installations, Central South University, Changsha 410083, China)

Abstract: Considering importance of study on physics fields and computer simulation for aluminum reduction cells so as to optimize design on aluminum reduction cells and develop new type of cells, based on analyzing coupled relation of physics fields in aluminum reduction cells, the mathematics and physics models were established and a coupled computation method on distribution of electric current and magnetic field, temperature profile and metal velocity in cells was developed. The computational results in 82 kA prebaked cells agree well with the measured results, and the errors of maxium value calculated for three main physics property fields are less than 10%, which proves that the model and arithmetic are available. So the software developed can be not only applied to optimization design on traditional aluminum reduction cells, but also to establishing better technology basis to develop new drained aluminum reduction cells.

Key words: aluminum reduction; reduction cells; computation of three fields; numerical simulation
CLC number: TF 111.52 **Document code:** A

1 COUPLED RELATION OF PHYSICS FIELD IN CELLS

There are six important physics fields in aluminum reduction cells[1-3], such as electric field, magnetic field, temperature field, flow velocity field, concentration field and stress field. The relations among these physics properties are shown as Fig. 1.

In regard to relation of six fields, electric field (electric current and potential distribution) is the energy foundation of operation and source of the other physics fields in reduction cells. Firstly, electric current causes the magnetic field and heat effect (Joule heat) which results in temperature field. On the one hand, disequilibrium of magnetic field distribution leads to electrolyte and molten aluminum flowing (forming flow velocity field). This causes Al_2O_3 and metals diffuse and deliquescence (forming concentration field), at the same time, bring the influence on forming frozen cryolite at the lining. On the other hand, temperature distribution is not only the foundation on forming cryolite freeze and guaranting reduction process, but also the important factor to influence energy equilibrium. It also results in thermal stress to distort cell structure, and influences melt motion and matter diffuseness. In a word, current efficiency, direct current consumption and cell life are determined by integrate effect of complicated relation among six physics fields. The previous studies showed that among six fields the electromagnetic field (the combined term of electric and magnetic field), temperature field and velocity field are the best important, which are called "three fields".

As there are intense coupling relationships among "three fields", in theory, the problems in reduction cells should be solved within coupled methods. Because of the complexity of the coupling relation and limitation of calculation method, it is impossible to realize coupled analysis of three fields, and at present all computation is carried out by separate (or partially separate) analyzing. In this paper, we will make a breakthrough on this aspect.

2 MATHEMATICS AND PHYSICS MODEL

The computational analysis techniques of "three fields" in aluminum reduction cells, which firstly emerged in 1970s, have developed some models and arithmetic methods. In this paper, the following models and arithmetic will be adopted by synthesizing recent achievements.

2.1 Current distribution in bus bar system[4]

According to Kirchhaff's law, current that is flowed by each part of bus bar system can be calcu-

① **Foundation item:** Project(G1999064903) supported by the National Key Fundamental Research and Development Program of China
Received date: 2002－04－16; **Accepted date:** 2002－07－01
Correspondence: ZHOU Nai-jun, Tel: +86-731-8836713; E-mail: njzhou@mail.csu.edu.cn

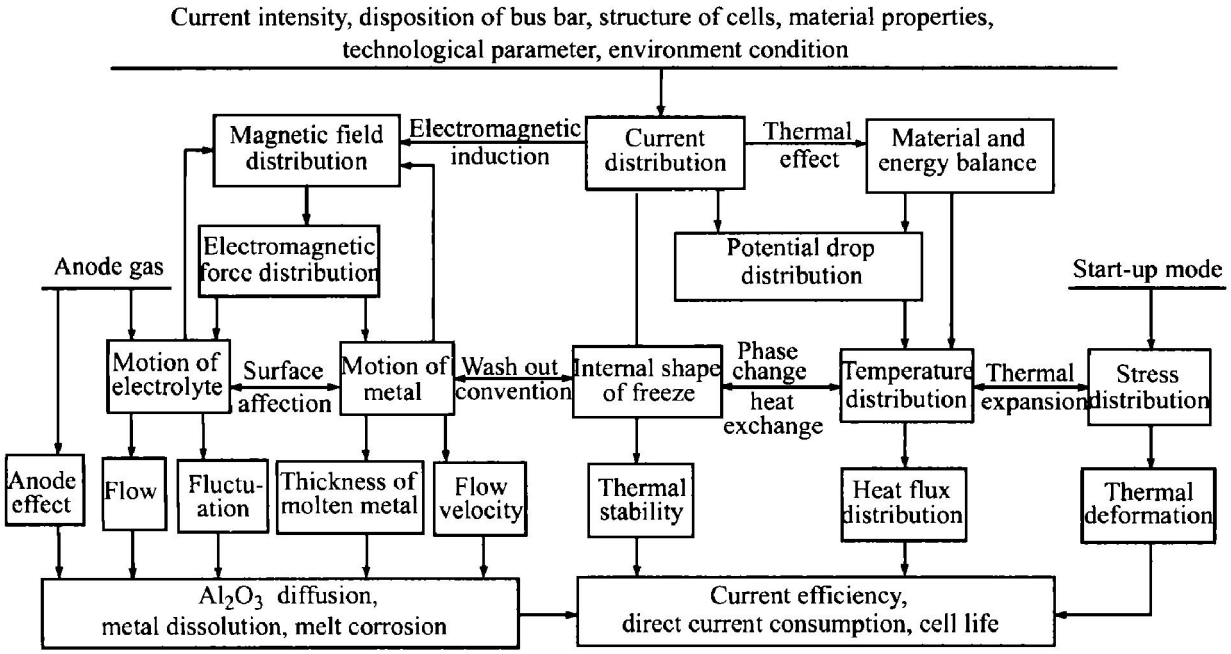

Fig. 1 Coupled relation of physics properties fields in aluminum reduction cells

lated. In calculation, the every section of bus bar is replaced by corresponding equivalent resistance on the basis of series-parallel connection relation among conductors of bus bar, by which a network chart of electric circuit will be obtained. Then electric potential on each node and current in bus bar may be computed with Kirchhoff's relational expression.

2.2 Computation model of magnetic field[5]

Magnetic field in aluminum reduction cells is composed of three parts including magnetic field induced by current in bus bar, magnetic field due to current in melt and carbon electrodes and magnetic field related to ferromagnet material.

Magnetic field induced by rectangle bus bar may be treated as superposition of the fields due to linear current. If axle of bus bar is defined as axis z by coordinate alternation, the magnetic induction intensity on point P outside bus bar can be written as

$$B=\int_{-a}^{a}\int_{-b}^{b}\frac{\mu_0 dx'dy'}{16ab\sum\sqrt{(x'-x)^2+(y'-y)^2}}\cdot\left(\frac{z_2}{\sqrt{(x'-x)^2+(y'-y)^2+z_2^2}}-\frac{z_1}{\sqrt{(x'-x)^2+(y'-y)^2+z_1^2}}\right)dx'dy' \tag{1}$$

where a and b are the width and height of fracture of the conductor, μ_0 is magnetic conductivity in vacuum. After this equation is computed by numerical integration method, using direction cosine of term $d\boldsymbol{z}\times d\boldsymbol{r}_0$[1], we can get the answer of components B_x, B_y, B_z.

Magnetic field due to current in carbon piece and melt can be computed with model of rectangle bus bar by dividing carbon piece and melt into several little rectangle units and supposing current in every little unit distribute equally.

Magnetic dipole method is adopted to calculate magnetic fields caused by ferromagnet material magnetizing. The model suggests that the magnetic fields induced by ferromagnet material in reduction cells are supposed to be substituted by the fields caused by several magnetic dipole in same place, and magnetization of magnetic dipole results from synthetical effect of two kinds of fields referring to the field induced by outer current and that due to ferromagnet material. At point P, the magnetic induction intensity caused by magnetic dipole can be expressed as[1, 5]

$$\boldsymbol{B}=\mu_0\boldsymbol{H}=\frac{\mu_0}{4\pi}\left|\frac{3(\boldsymbol{P}_m\cdot\boldsymbol{r})\boldsymbol{r}}{r^5}-\frac{\boldsymbol{P}_m}{r^3}\right| \tag{2}$$

Depending on above equations, magnetic induction intensity at any point is obtained by superposition principle. Then the electromagnetic forces, $\boldsymbol{F}$, can be determined by the cross product between current density vector, $\boldsymbol{J}$, and magnetic field vector, $\boldsymbol{B}$, which is also shown as $\boldsymbol{F}=\boldsymbol{J}\times\boldsymbol{B}$. The components of electromagnetic forces at x, y and z directions are written as[1]

$$F_x=J_yB_z-J_zB_y,\quad F_y=J_zB_x-J_xB_z,$$
$$F_z=J_xB_y-J_yB_x$$

2.3 Computation model of temperature field

Computation analysis method in the area from carbon anode to cathode (including the melt between poles) is to connect electric conduction equation with heat conduction equation to compute current field and temperature field.

2.3.1 Control equation[1, 6]

Electric conduction differential equation:

$$\nabla \cdot (\sigma \nabla V) = 0 \quad (3)$$

Heat conduction equation:

$$\nabla \cdot (\lambda \nabla T) + q_{vol} = 0 \quad (4)$$

where σ is electric conduction rate related to temperature, V is potential difference, T is temperature, λ is heat conduction coefficient, and q_{vol} is Joule heat of control unit, which is omited in unconduction section.

2.3.2 Boundary condition

1) Boundary conditions of electric conduction equation:

a. Electric potential at molten aluminum surface or cathode carbon surface is iso-potential, and electric potential in molten aluminum layer is evenly distributed.

b. As unconduction on side ledge of the cells, all of current pass through carbon cathode.

c. Cathode clubs share all of the current in cells equally.

2) Boundary conditions of heat conduction equation:

a. In the electrolyte and molten aluminum layer, the temperature is equal in every place, which can be obtained by measuring.

b. The interface between upper protective layer of frozen cryolite and anode is treated as adiabatic plate.

c. Surrounding temperature can be given by detecting in workshop.

d. The temperature on contact point between cathode bus bar and soft bus bar is also given by measuring.

e. Based on model and calculating method listed in references, other parameters can be obtained, including coefficient of heat dissipation at outside surface of the freeze, heat transfer coefficient at the interface between molten aluminum and carbon cathode, heat transfer coefficient at the interface between molten aluminum and side freeze, primary crystal temperature of electrolyte, and so on. Physics properties data of materials originate from factory or references. It has been discussed in detail in Refs. [7 - 10].

As coupling of equation and nonlinearity of physics parameter, numerical method is the only solution to Eqns. (3) and (4). At present, the finite difference method is frequently adopted and "slice" model[1] is available to resolve the problem in practice.

2.4 Computation model of metal velocity field

Using Reynolds mean Navier-Stocks equation group, three-dimensional turbulent motion of melt may be described. In general, it is necessary to put emphasis on studying flow of molten aluminum. If following hypotheses are suggested:

1) Regarding melt flow in aluminum reduction cells as a steady state and incompressible flow;

2) Supposing molten aluminum surface is free surface (ignoring viscous force on the surface)[13].

We will gain control equation[11, 12]:

Continuity equation

$$\frac{\partial(\rho u_i)}{\partial x_i} = 0 \quad (5)$$

Momentum equation

$$\frac{\partial}{\partial x_i}(\rho u_i u_j) = -\frac{\partial p}{\partial x_j} + \frac{\partial}{\partial x_i}\left[\mu_{eff}\left(\frac{\partial u_j}{\partial x_i} + \frac{\partial u_i}{\partial x_j}\right)\right] + \rho g_j + F_j \quad (6)$$

where u represents melt velocity and x is coordinate direction (i, j = 1, 2, 3, represent three directions of x, y, z), ρ is melt density, g_i is component of acceleration due to gravity, F_j is component of volume force effecting on melt (consisting of electromagnetic force and floatage), μ_{eff} is effective viscosity (being equal to sum of molecule viscosity and turbulent viscosity, which can be expressed as $\mu_{eff} = \mu + \mu_T$).

Turbulent kinetic energy equation and equation of rate of turbulent kinetic dissipation are required to close $k-\varepsilon$ double-equation model describing turbulent flow[12].

$$\frac{\partial}{\partial x_i}(\rho k u_i) = \frac{\partial}{\partial x_i}\left[\left(\mu + \frac{\mu_T}{\sigma_k}\right)\frac{\partial k}{\partial x_i}\right] + \mu_T \frac{\partial u_j}{\partial x_i}\left(\frac{\partial u_i}{\partial x_j} + \frac{\partial u_j}{\partial x_i}\right) - \rho\varepsilon \quad (7)$$

$$\frac{\partial}{\partial x_i}(\rho \varepsilon u_i) = \frac{\partial}{\partial x_i}\left[\left(\mu + \frac{\mu_T}{\sigma_\varepsilon}\right)\frac{\partial \varepsilon}{\partial x_i}\right] + C_1 \frac{\varepsilon}{k}\mu_T \frac{\partial u_j}{\partial x_i}\left(\frac{\partial u_i}{\partial x_j} + \frac{\partial u_j}{\partial x_i}\right) - C_2 \rho \frac{\varepsilon^2}{k} \quad (8)$$

$$\mu_T = C_\mu \rho k^2 / \varepsilon \quad (9)$$

where C_μ = 0.09, C_1 = 1.44, C_2 = 1.92, σ_k = 1.0, σ_ε = 1.3[12].

Based on the mixed difference format derived from finite volume method, the partially differential equations will straggle to iteratively calculate them according to alternating mesh and modified SIMPLE method. After computing velocity and pressure distribution, the height of molten aluminum surface may be obtained by the following expression[13]:

$$p + \rho_m g h = C_i \quad (10)$$

where p is static pressure, h is height from molten aluminum bottom to upper surface, ρ_m is density of molten aluminum, C_i is constant.

3 COUPLED COMPUTATION METHOD

By analyzing coupled relations of physics fields, current in bus bar is calculated independently. After that, it is easy to deduce the result of magnetic field due to bus bar current and ferromagnet material with generally considering the influence of each adjacent cells. In regard of anode block and part of cell body under it, the coupled computation method must be adopted for computing the current distribution and

temperature distribution. According to different anode height in practical cells (as existing different current), this method draws slice from each anode for obtaining current density, temperature distribution and the freeze of cryolite in the lining in different place. Then magnetic fields due to carbon piece and melt are also computed. Computing the metal velocity distribution is a complex process. Firstly, on the basis of velocity distribution and synthesis magnetic field calculated previously, we should simulate electromagnetic force field and then obtain flow velocity of metal; and because there is important influence on analysis result of temperature, which is related to flow velocity of molten aluminum and its scour act, it is necessary for returning computational results to calculate magnetic field and electro-thermal fields again. In general, this process will repeat 3 ~ 5 times, then convergence answers can be found out. Lastly, when the interface height of molten aluminum is calculated out, the computation procedure is completed. The whole computation process is shown as Fig. 2.

4 COMPUTATION INSTANCE

4.1 Object and parameters

To prove the computational model availability, measurement and simulation calculation were performed in 82 kA prebaked anode cells. The series of this type cells were reformed from traditional 60 kA side interposing cells. They inherit from former cell shell and previous disposition with entering current from two points on single end, but succeed in adopting third point for compensation on side A and substitute dry material of impervious barriers for refractory brick layer. The structure and primary technological parameters are listed in Table 1.

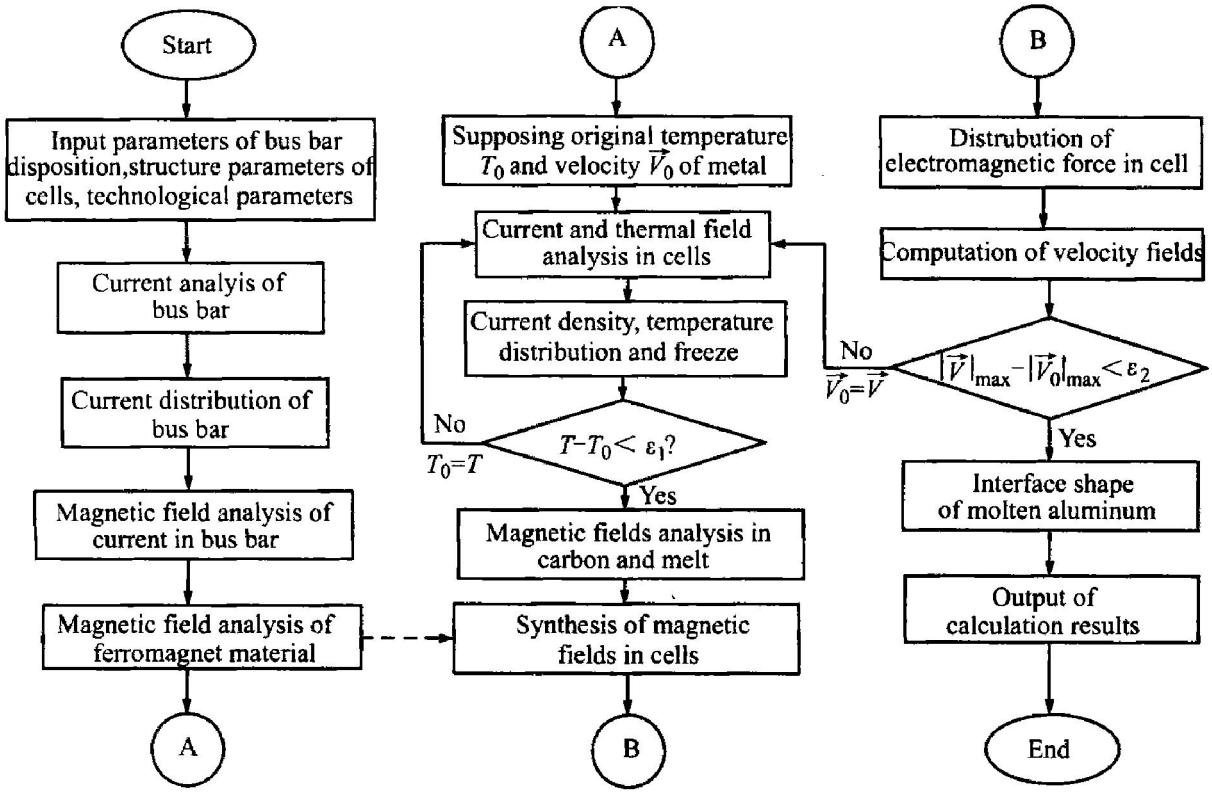

Fig. 2 Computation procedure of physics fields in aluminum reduction cells

Table 1 Structure and technological parameters in 82 kA prebaked anode cells

Primary structure size	Primary technological parameter
Size of cell tank: 5.40 m × 2.94 m × 0.50 m	Series current: 82.0 kA
Length of carbon anode: 1.160 m	Cell potential: 4.27 V
Height of carbon anode: 0.540 m	Height of electrolyte: 20.0 cm
Height of carbon cathode: 0.400 m	Height of melt aluminum: 20.0 cm
Thickness of dry impervious barriers: 0.161 m	Temperature of electrolyte: 960 ℃
Thickness of refractory brick: 0.134 m	Temperature of molten metal: 955 ℃
Thickness of asbestos board: 0.060 m	Distance between poles: 4.0 cm
Thickness of calcium silicate plate: 0.010 m	Surroundings temperature of cell side: 50 ℃
Section of cathode club: 0.130 m × 0.130 m	Surroundings temperature of cell bottom: 35 ℃
Thickness of side carbon piece: 0.115 m	Primary crystal temperature of electrolyte: 935 ℃
Height of side carbon piece: 0.550 m	Current efficiency: 91.5%

4.2 Calculation results

During coupled analysis, the software developed by ourselves was used to compute current, magnetic and thermal fields; and the large commercial software CFX which was developed second time was used to compute the velocity field. Data between two kinds of software are exchanged by data file. The simulated results are shown as Figs. 3 – 7, in which the data location is in the layer of molten aluminum 10 cm upper from cathode surface.

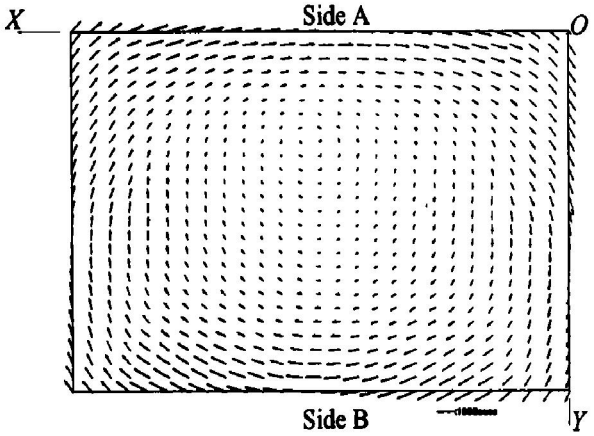

Fig. 3 Distribution of horizontal magnetic field in 82 kA prebaked anode cells

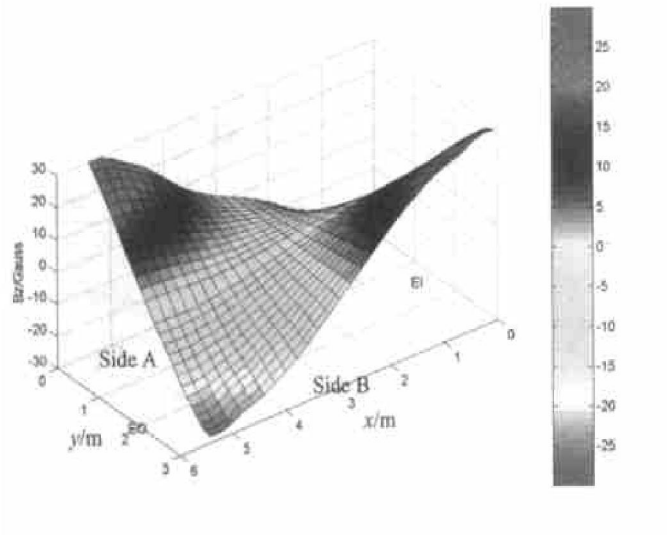

Fig. 4 Distribution of vertical magnetic field in 82 kA prebaked anode cells

4.3 Comparison between measured value and calculation results

Tables 2 and 3 indicate that the simulated results of magnetic and metal velocity field agree with the measured results at most measured positions, and the errors of maxium value calculated for three main physics property fields are less than 20%. However, the internal shape of freeze is incline to be ideal,

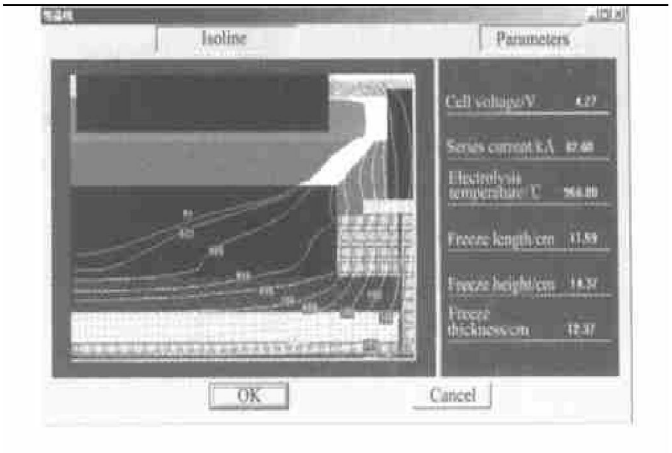

Fig. 5 Isoline of temperature and freeze profile in 82 kA prebaked anode cells

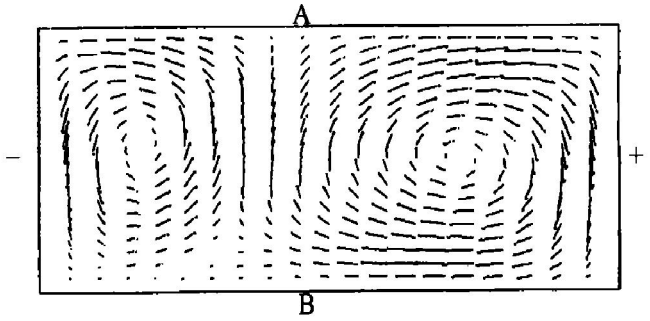

Fig. 6 Vector chart of horizontal velocity in 82 kA prebaked anode cells

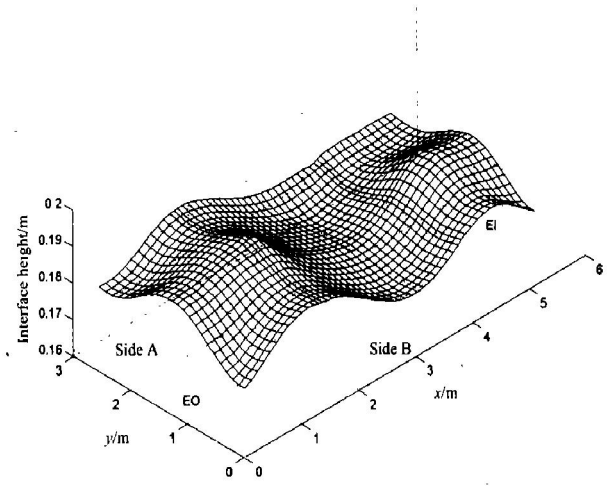

Fig. 7 Interface shape of melt metal in 82 kA prebaked anode cells

which shows large height and thickness and short stretching leg. The deviation is attributed to: 1) inaccuracy of orientation about measured positions; 2) measuring error; 3) current and potential fluctuate during measure; 4) influence on internal shape of freeze; 5) error with selecting physics parameters.

Table 2 Comparison between measured value and calculated results

Measured position	Coordinate of position/m			Measured value of magnetic induction / 10^{-4}T			Calculated value of magnetic induction / 10^{-4}T			Velocity of molten aluminum/ ($cm \cdot s^{-1}$)				
										Measured	Calculated			
	x	y	z	B_x	B_y	B_z	B_x	B_y	B_z	V	V_x	V_y	V_z	V
1	0.875	0.2	0.875	−65.16	28.96	−19.9	−59.08	21.51	−21.07	10.77	−13.3	0.3	−0.3	13.3
2	1.54	0.2	0.875	−57.6	13.7	−13.9	−52.53	15.74	−12.18					
3	2.205	0.2	0.875	−43.2	13.7	−6.7	−48.88	6.21	−4.37	10.94	−12.3	−2.0	−0.2	12.5
4	2.785	0.2	0.875	−63.5	−1.3	−2.7	−49.47	−0.68	0.72					
5	3.365	0.2	0.875	−41.7	−3.4	6.7	−49.94	−7.81	6.09	12.17	9.6	−2.6	−0.1	9.9
6	3.945	0.2	0.875	−72.4	−21.9	13.3	−58.72	−16.44	13.36					
7	4.525	0.2	0.875	−67.2	−11.5	19.9	−62.08	−20.99	21.06	12.87	12.3	−0.4	−0.3	12.3
8	5.2	0.4	0.875	−42.2	−40.7	16.4	−33.97	−41.44	22.60	11.12	5.1	6.1	0.4	8.4
9	5.2	1.49	0.875	3.0	−36.7	−4.8	−1.45	−43.64	−5.07	11.99	0.2	14.4	−0.2	14.5
10	5.2	2.78	0.875	34.5	−46.5	−16.9	20.88	−47.92	−28.45	10.77	−2.0	7.3	0.1	7.6
11	4.525	2.78	0.875	61.5	−29.6	−27.5	65.80	−31.65	−27.33	10.41	−7.2	1.0	0.0	7.3
12	3.860	2.78	0.875	64.9	−25.1	−14.9	69.94	−36.13	−20.04					
13	3.195	2.78	0.875	71.5	−15.57	−5.2	65.86	−15.36	−9.22	11.99	−9.4	−0.8	−0.1	9.5
14	2.615	2.78	0.875	60.9	0.5	3.26	65.55	2.23	1.74					
15	2.035	2.78	0.875	82.5	17.4	10.0	63.64	19.59	12.42	10.6	12.4	−0.5	−0.2	12.4
16	1.455	2.78	0.875	72.2	27.0	13.0	66.49	31.82	16.18					
17	0.875	2.78	0.875	61.9	35.6	18.3	62.44	40.12	23.33	10.94	9.7	1.8	−0.3	9.9
18	0.2	2.5	0.875	52.2	58.6	23.6	46.86	48.05	28.45	10.24	1.7	7.6	−0.1	7.8
19	0.2	1.49	0.875	7.5	56.1	−5.8	3.94	50.57	−5.06	12.87	−6.0	14.6	−0.1	15.7
20	0.2	0.4	0.875	−49.2	46.6	−24.2	−39.55	41.56	−22.60	10.41	−1.5	9.6	0.6	9.7

Use three-dimension gauss meter to measure magnetic induction intensity in molten aluminum layer, and flow velocity of molten aluminum is detected with iron club melting method (every point measures three times, and results are average value).

Table 3 Contrast between measured and calculated characteristic parameters of freeze in cells

Item	1011# cell		2030# cell		2042# cell		Designed condition
	Calculated	Measured②	Calculated	Measured②	Calculated	Measured②	
Temperature of electrolyte / ℃	966.4①	966.4	956.0①	956.0	968.4①	968.4	960
Primary crystal temperature of electrolyte / ℃	930	–	925	–	940	–	935
Length of freeze / cm	9.24	12.6	11.25	14.4	14.41	17.6	11.59
Height of freeze / cm	11.96	8.2	12.02	9.0	15.57	11.2	14.37
Width of freeze / cm	12.94	10.8	13.01	11.2	13.09	12.2	12.37

① Computed by measured temperature; ② arithmetic mean value of measured values.

5 CONCLUTIONS

1) By analyzing coupled relation of physics fields in aluminum reduction cells, the coupled analysis methods on electromagnetic field, thermal field and flow field of aluminum are put forward, and the series of computation softwares are developed.

2) The computational results on physics fields agree with measured results in 82 kA prebaked cells, indicating that the developed software can be applied to simulation computation on three-dimensional physics field in aluminum reduction cells.

REFERENCES

[1] MEI Chi. Simulation and Optimization on Nonferrous Metallurgy Furnace[M]. Beijing: Metallurgical Industry Press, 2001. 131-174. (in Chinese)

[2] Tabsh I, Dupuis M, Gomes A. Process simulation of aluminum reduction cells[J]. Light Metals, 1996: 451-457.

[3] Bos J. Numerical simulation, tools to design and optimize smelting technology[J]. TMS Light Metals, 1998: 393-401.

[4] Dupis M. Computation of accurate horizontal current density in metal pad using a full quarter[J]. TMS Light Metals, 2000: 169-178.

[5] Sele T. Computer model for magnetic fields in electrolytic cells including the effect of steel ports[J]. Light Metal, 1991: 393-398.

[6] Dupuis M. Thermo-electric design of a 400 kA cell using mathematical models[J]. Light Metals, 2000: 297-302.

[7] Solhiem A. Heat transfer coefficients between bath and side ledge in aluminum cells[J]. Light Metals, 1983: 425.

[8] Dupuis M, Tabsh I. Using a steady-state model of an aluminum reduction cell to investigate the impact of design changes[J]. Light Metal, 1996: 417-429.

[9] Bruggeman J N, Danka D J. Two dimensional thermal modelling of the Hall-Heroult cell[J]. Light Metals, 1990: 203-209.

[10] YOU Wang, WANG qian-pu, MEI Chi. On-line dynamic simulation of freeze profile in aluminum electrolysis[J]. The Chinese Journal of Nonferrous Metals, 1998, 8(4): 695-699. (in Chinese)

[11] HUANG Zhao-lin, YANG Zhi-feng, WU Jiang-hang. Numerical simulation of turbulent flow and melt topography in aluminum reduction cells[J]. Chinese Journal of Computational Physics, 1994, 11(2): 179-184. (in Chinese)

[12] SUN Yang, FENG Nai-xiang. Numerical calculation of flow field in 186 kA large prebaked anode aluminum reduction cell[J]. Chinese Journal of Rare Metals, 2001, 25(5): 382-385. (in Chinese)

[13] Davidson P A, Lindsay R I. A new model of interfacial waves in aluminium reduction cells[J]. Light Metals, 1997: 437-442.

(Edited by YUAN Sai-qian)